

1 A polyetic modelling framework for plant disease emergence

2

3 Laetitia Willocquet^{a1,*}, S. Savary¹, B.A. McDonald², A. Mikaberidze^{2,3}

4

5 ¹AGIR, INRAE, Université de Toulouse, INPT, INP-EI Purpan, Castanet-Tolosan, France

6 ²Plant Pathology, Institute of Integrative Biology, Zurich (IBZ), ETH Zurich, LFW B16, 8092 Zurich, Switzerland

7 ³Current address: School of Agriculture, Policy and Development, University of Reading, Whiteknights, Reading,

8 RG6 6AR United Kingdom

9 * Corresponding author. Email: Laetitia.willocquet@inra.fr

10

11 Abstract

12 Plant disease emergences have dramatically increased recently as a result of global changes, especially with
13 respect to trade, host genetic uniformity, and climate change. A better understanding of the conditions and
14 processes determining epidemic outbreaks caused by the emergence of a new pathogen, or pathogen strain, is
15 needed to develop strategies and inform decisions to manage emerging diseases. A polyetic process-based
16 model is developed to analyse conditions of disease emergence. This model simulates polycyclic epidemics
17 during successive growing seasons, the yield losses they cause, and the pathogen survival between growing
18 seasons. This framework considers an immigrant strain coming into a system where a resident strain is already
19 established. Outcomes are formulated in terms of probability of emergence, time to emergence, and yield loss,
20 resulting from deterministic and stochastic simulations. An analytical solution to determine a threshold for
21 emergence is also derived. Analyses focus on the effects of two fitness parameters on emergence: the relative
22 rate of reproduction (speed of epidemics), and the relative rate of mortality (decay of population between
23 seasons). Analyses revealed that stochasticity is a critical feature of disease emergence. The simulations
24 suggests that: (1) emergence may require a series of independent immigration events before a successful

25 invasion takes place; (2) an explosion in the population size of the new pathogen (or strain) may be preceded by
26 many successive growing seasons of cryptic presence following an immigration event, and; (3) survival between
27 growing seasons is as important as reproduction during the growing season in determining disease emergence.

28

29 KEYWORDS

30 disease emergence, process-based model, pathogen fitness, polyetic epidemics, pathogen survival

31

32 1. INTRODUCTION

33 The emergence of disease in plant populations has important impacts on both agricultural production and
34 natural ecosystems (Anderson *et al.*, 2004; Lucas, 2017). While emerging plant diseases threaten biodiversity
35 and the entire range of services contributed by plants to the biosphere (Anderson *et al.*, 2004), the emergence
36 of plant diseases constitutes an immediate threat to food security, from local to global scales, because of the
37 losses in production, and also because losses to plant disease affect food access (economic or physical) and the
38 quality of food (Savary *et al.* (2017). The literature provides growing evidence that plant disease emergences
39 have dramatically increased recently, as a result of global changes in trade, host genetic uniformity, and climate
40 (Anderson *et al.*, 2004; Fisher *et al.*, 2012; McDonald and Stukenbrock, 2016; Paine *et al.*, 2016).

41 A relatively recent example of emergence of new pathogen strains is the introduction into Europe of a
42 strain carrying the A2 mating type of *Phytophthora infestans*, the causal agent of potato late blight
43 (Zwankhuizen and Zadoks, 2002; Lucas, 2017). The emergence of this strain and its lineages, both resistant to
44 metalaxyl and more aggressive, led to more diversified, sexually reproducing, pathogen populations, and
45 increased disease intensity in Europe (Goodwin *et al.*, 1996). Stem rust of wheat is another example. Stem rust
46 epidemics, which were common in the USA during the first half of the last century, became rare after the
47 pathogen (*Puccinia graminis* f. sp. *tritici*) was controlled by combining the deployment of new resistance genes
48 in wheat varieties with the eradication of barberry, which is the alternate host on which the pathogen

49 reproduces sexually (Roelfs, 1978; 1985). In 1998, new races of this pathogen (called Ug99) were detected in
50 Uganda that were virulent against resistance genes present in wheat varieties widely grown in East Africa,
51 leading to local but severe epidemics in the region (Singh *et al.*, 2015). International efforts to generate and
52 deploy resistant varieties helped to limit impacts from races of these new lineages (Singh *et al.*, 2015), but the
53 recent detection of stem rust in different parts of Europe is now threatening wheat production in this part of
54 the world (Saunders *et al.*, 2019). A third and recent example of strain introduction is that of *Puccinia striiformis*
55 f. sp. *tritici*, the causal agent of stripe (yellow) rust of wheat, into North-Western Europe in 2011 (de Vallavieille-
56 Pope *et al.*, 2018) which caused serious epidemics.

57 An example of emergence of a new pathogen is *Pyricularia graminis-tritici*, the cause of wheat blast.
58 The disease was restricted to South America until 2016, when the pathogen was accidentally introduced and
59 caused a severe outbreak in South Asia (Ceresini *et al.*, 2018). Another example of new pathogen emergence is
60 the Asian soybean rust, caused by *Phakopsora pachyrhizi*, which was introduced into South America at the
61 beginning of this century and has since severely impacted soybean production on that continent (Lucas, 2017).
62 Rhizomania is a virus disease of sugar beet that was first detected in the United Kingdom in 1987 and has since
63 spread, resulting in increasing numbers of epidemics (Gilligan *et al.*, 2007). Other recent examples of disease
64 emergence with very disastrous impacts on perennial crops include huanglongbing on citrus in the New World
65 (Gottwald, 2010) and *Xylella fastidiosa* on olive trees in Southern Europe (Saponari *et al.*, 2019).

66 Disease emergence may be associated with changes in the environment, especially, human-made
67 changes. A much-debated example is the case of fusarium head blight of wheat (wheat scab), which has been
68 associated with the maize-wheat rotation, and with no-till practices (Zadoks and Schein, 1979; McMullen *et al.*,
69 2012). Another example is that of false smut of rice, which has been associated with the cultivation of hybrid
70 rice (Savary *et al.*, 2017). A third example of environmental change-driven emergence is that of *Sclerotium*
71 *rolfsii*, a tropical pathogen on legumes (among many other hosts) becoming prevalent in the state of New York
72 as a result of warming climate (S. Pethybridge, Personal Communication).

73 In their seminal article, Heesterbeek and Zadoks (1987) proposed a mathematical theory of pandemics,
74 with three phases: zero-order, first-order, and second-order epidemics. This theory considers two groups of
75 processes, the spatial spread of disease and the accumulation of disease cycles within and across crop cycles, to
76 analyse pandemics. While the zero-order epidemic is field-bound and polycyclic, the first-order epidemic is
77 area-bound and polycyclic, and the second-order is both continental and polyetic. The present article is a
78 response, some thirty years later, to this article. Figure 1 represents a synthesis of processes which may be
79 associated with disease emergence, organised in three paths. Path 1 is the invasion of a new pathogen into an
80 ecosystem, through introduction, establishment, and spread. Path 1 is exemplified by the wheat blast epidemic
81 in Bangladesh. Path 2 is the emergence of disease in response to environmental changes in an ecosystem,
82 where environmental changes lead to disease intensification, further leading to disease spread within entire
83 (agro)systems. Path 2 is illustrated by fusarium head blight of wheat or false smut of rice. Path 3 is the
84 emergence of new strains through evolutionary processes. Path 3 is illustrated by wheat stem rust in Sub-
85 Saharan Africa. Emergence paths may be combined. For instance, Paths 1 and 3 are combined in the potato late
86 blight epidemic of the 1990s in Western Europe; Paths 1, 2, and 3 are combined in the emergence of stripe rust
87 in Western Europe.

88 Similar to the emergence and re-emergence of infectious diseases in humans (Wilcox and Collwell,
89 2005), the emergence of plant diseases entails the consideration of biocomplexity, i.e., of complex systems,
90 where the biology of pathogens and hosts, their genetics, the changing environments - both natural and
91 human-made, and the social and economic structures (including plant health management systems) interact.
92 The present analysis does not address the biocomplexity of plant disease emergence as a whole, but rather
93 focuses on a fragment of Figure 1, with emphasis on Paths 1 (emerging pathogens) and 3 (emerging strains).
94 Elements of Path 2 (environmental change) are subsumed in the form of stochastic features of the modelling
95 work.

96 Here we present a series of hypotheses underpinning the processes at play in disease emergence.

97 These hypotheses involve both demography (epidemiology) and population genetics as follows:

98 (1) from an epidemiological standpoint, emergence is a polyetic process, i.e., it is a process spanning several
99 consecutive crop seasons (Zadoks, 1974; Zadoks and Schein, 1979; Heesterbeek and Zadoks, 1987);

100 (2) this polyetic process is inherently stochastic because it entails random and abrupt changes in the pathogen
101 and host populations (Shaw, 1994). The process is also affected by random fluctuations in the environment
102 (Gilligan and Van den Bosch, 2008);

103 (3) an important determinant of successful emergence is the diversity in the population from which the
104 emerging pathogen originates. We assume the pathogen (or pathogen strain) to be sampled by chance in a
105 large genetic pool. The more diverse this pool, the higher the likelihood of fit to a given biological (hosts) and
106 physical setting (McDonald and Stukenbrock, 2016);

107 (4) pathogen migration (introduction) is often the primary mechanism associated with disease emergence
108 (McDonald and Stukenbrock, 2016);

109 (5) the level of crop losses associated with epidemics constitutes a useful metric for the impact of disease
110 emergence (Savary *et al.*, 2006; 2017; 2019).

111 A range of models have been developed to analyse the dynamics of epidemics or pathogen populations
112 over multiple crop seasons. Leonard (1977) analysed the dynamics of plant pathogen genotypes over seasons
113 to investigate plant pathogen evolution under the gene-for-gene hypothesis. Since then, several polyetic
114 models have considered cycles of epidemic processes (disease transmission in the presence of the host)
115 followed by survival processes (pathogen decay in the absence of the host). Several models have considered
116 one pathogen genotype in order to address, e.g., thresholds for persistence according to epidemiological
117 parameters (e.g., Gubbins *et al.*, 2000; Madden and Van den Bosch, 2002), whereby persistence corresponds to
118 disease emergence caused by invasion. These models were expanded to consider two pathogen genotypes to
119 analyse the evolutionary dynamics of pathogen populations (Van den Berg *et al.*, 2011; Hamelin *et al.*, 2011).

120 Comparatively fewer stochastic polyetic models have been developed, showing chaotic polyetic patterns (Shaw,
121 1994), or guiding management strategies (with a spatially explicit stochastic model of sugar beet rhizomania;
122 Gilligan *et al.*, 2007). To our knowledge, no model has yet been developed which simultaneously accounts for
123 polyetic processes, stochasticity, and the occurrence of several pathogen genotypes. Furthermore, none of the
124 polyetic models reported so far explicitly accounts for the impact of disease on yield loss.

125 The objectives of this work were to: (1) design a modelling framework to better define the conditions
126 determining disease emergence, (2) illustrate the use of the model by considering fitness components that
127 characterize the growth of the pathogen population during the growing season and its survival between
128 growing seasons and analysing their effects on disease emergence, and (3) draw some conclusions on
129 properties associated with disease emergence.

130

131 2. MATERIALS AND METHODS

132 2.1 Model requirements

133

134 Model specifications were established to build a structure incorporating processes related to population
135 genetics, epidemiology, and crop losses in order to analyse the conditions associated with disease emergence
136 and its effects on yield. The model and the outcomes of the analysis apply equally well to: (i) the situation when
137 a strain of a new pathogen is emerging on the background of another, resident pathogen population infecting
138 the same host, and (ii) the situation where a new, immigrant strain of a pathogen emerges on the background
139 of an already established population of the same pathogen. For the sake of simplicity, we will only refer to the
140 second situation below. The following requirements for the model were identified:

- 141 • Because disease emergence takes place over several crop seasons (Gilligan and Van den Bosch, 2008),
142 the model generates dynamics of epidemics and pathogen survival over successive cropping cycles, i.e.,

143 it encapsulates *polyetic processes* (Zadoks, 1974; Zadoks and Schein, 1979; Heesterbeek and Zadoks,
144 1987).

- 145 • Epidemics of many plant diseases entail secondary infections occurring during a crop season. The
146 model therefore considers *polycyclic epidemics* within crop seasons.
- 147 • The model involves *different strains of a pathogen* in order to account for the evolutionary processes
148 involved in disease emergence.
- 149 • Disease emergence often originates from the *migration* of a new pathogen (Fig. 1, Path 1), or of a new
150 pathogen strain (Fig. 1, Path 3), into an agrosystem. The model therefore incorporates an immigration
151 process.
- 152 • Modelling of the dynamics of *primary inoculum* with varying numbers of propagules, originating from
153 preceding crop seasons and/or from immigration, and decaying over time, is a requirement, because (1)
154 primary inoculum enables the initiation of seasonal epidemics, (2) a migrating pathogen strain enters
155 the system as primary inoculum, and (3) primary inoculum also constitutes the link between two
156 seasonal epidemics, and therefore provides the bridge needed to consider polyetic epidemics.
- 157 • *Crop losses* are an essential feature of epidemics in agroecosystems. The model therefore translates
158 multi-seasonal, polyetic epidemics into their impact on crop performance as yield losses.

159

160 2.2 Model description

161 The system considered in the model is 1 m² of a crop, under the "mean-field" hypothesis: the system
162 considered is surrounded by systems with the same features and dynamics. This 1 m²-system and its
163 surroundings are repeated in successive crop seasons separated by off-seasons. During any crop season, this
164 system and its neighbours are considered in a steady-state relationship. In particular, incoming and outgoing
165 inoculum between these systems cancel each other out, so that the net inflow/outflow balance is null. The

166 model time step is one day, so as to accommodate processes which can have fast dynamics, such as polycyclic
167 processes.

168 We consider a crop that is grown in regular cropping cycles (Supplementary Figure 1). Each cropping
169 cycle consists of the period when the crop is present (crop season) and the period when the crop is absent (off-
170 season). The crop season starts from crop planting and ends at harvest, and has two phases: the crop
171 establishment phase and the crop growth phase (or, shortly, the growing season). The duration of each of the
172 two phases (*CEP*, crop establishment period, and *CGP*, crop growth period) can vary depending on the crop,
173 crop type (winter or spring crop) and location. Simulations start at crop planting, and are run for 30 cropping
174 cycles.

175 The model considers one host plant genotype, e.g. a variety of a given crop, which can be infected by
176 two strains of a given pathogen: a local (or resident) strain and an exogenous (or immigrant) strain. The local
177 pathogen strain is present at the beginning of the simulation, while the exogenous pathogen strain is
178 introduced into the system during the course of the simulation. The local population consists of strains that are
179 already well adapted to local conditions. This local population is represented in the model by one local strain
180 which has fixed demographic parameters. The exogenous population is established in a range of conditions
181 (outside from the system), which may differ from the conditions of the considered system. This population is
182 therefore more diverse, and generally less well adapted to the local conditions of the system. It thus consists of
183 strains with a broader range of fitness attributes compared to the local population. This exogenous population
184 is represented in the model by one strain with a fitness that can vary over cropping cycles. This variation
185 reflects the hypothesis that the exogenous strain is less well adapted to the local conditions than the resident
186 strain, and therefore is less well adapted to the environmental variations over cropping cycles. Each cropping
187 cycle therefore involves two strains of the pathogen, the (fixed) local strain, and the (variable, random)
188 exogenous strain.

189 Each cropping cycle involves several processes, which are represented as rates (Forrester, 1961; Savary
190 and Willocquet, 2014) in Figure 2. These are the processes involved in the development of epidemics, including
191 primary and secondary infections: RI (rate of infection); processes involved in the survival and decay of
192 inoculum: $Rdecay$ (rate of inoculum decay); and processes involved in yield losses incurred from disease: RL
193 (rate of loss). These processes are next described in greater detail. The model variables and parameters are
194 described in Table 1.

195 In each cropping cycle, the epidemic starts with primary infections (RPI), which take place at the end of
196 the crop establishment phase, as the crop growth phase starts. Primary infections have two origins. First,
197 primary infections can originate from inoculum produced from epidemics which took place in previous crop
198 seasons (polyetism), and second, primary infections can result from incoming inoculum (immigration from an
199 exogenous population). In the beginning of the crop growth phase, the rate of primary infections for each
200 strain, $j = 1$ (local), or 2 (immigrant), is therefore written as:

$$201 \quad RPI_j = convSP \times S_j + RM_j \quad (1)$$

202 Where $convSP$ is the conversion of surviving inoculum into a rate of primary infections; S_j is the number of
203 surviving propagules for each strain; and RM_j is the rate of infections originating from immigrant strains,
204 referred to as the rate of immigration. The rate of primary infections, RPI_j , has the value given by Eq. (1) only on
205 the first time step of each growing season and is set to zero at all other times.

206 An epidemic takes place as the injury level, i , increases according to a logistic curve (exponential
207 increase of secondary infections, limited by the carrying capacity of the host crop) with a relative rate of
208 growth, RRg . As the seasonal epidemic unfolds, interaction between strains takes place, in the form of
209 competition towards host (crop) sites. This interaction between strains accounts for the maximum possible level
210 of injury (carrying capacity) at a given time, considering all plant sites occupied by the different strains at this
211 time. The rate of infection of each strain j , comprising primary and secondary infections, is therefore written as:

$$212 \quad RI_j = [RRg_j \times i_j \times (1 - ((i_1 + i_2) / imax))] + RPI_j + starter_j \quad (2)$$

213 where RRg_j is the relative rate of injury increase for strain j ; i_j is the injury level of strain j ; i_1 is the injury level
214 caused by the local strain; i_2 is the injury level caused by the immigrant strain; $imax$ is the carrying capacity of
215 injury, i.e., the maximum level of injury; RPI_j is the rate of primary infections associated with strain j ; and $starter_j$
216 is the number of primary infections at the beginning of the multiple-cropping cycle simulation (this parameter is
217 non-zero only during the first time step of the cropping cycle 1).

218 At the end of a cropping cycle, the terminal injury level (i_j) is converted into surviving inoculum, S_j , for
219 each of the two strains. The number of surviving propagules decreases over time according to a negative
220 exponential dynamics, at a speed proportional to a relative rate of decay (RRD_j):

$$221 \quad Rdecay_j = RRD_j \times S_j, \quad (3)$$

222 where $Rdecay_j$ is the rate of decay of surviving propagules of strain j ; RRD_j is the relative rate of decay of
223 surviving propagules of strain j , and S_j is the number of surviving propagules of strain j .

224 Injuries impair the physiological processes involved in crop growth and yield build-up, ultimately
225 leading to yield losses. The several possible damage mechanisms from injuries are represented in a very
226 simplified manner by a single rate of yield loss, RL , which increases proportionally to the running level of
227 combined injuries caused by both strains, $i_1 + i_2$:

$$228 \quad RL = RRL \times (i_1 + i_2) \times [1 - (YL / Ya)] \quad (4)$$

229 where RRL is the relative rate of yield loss; i_1 and i_2 are the injury levels from the local and immigrant strains,
230 respectively; YL is the yield loss, i.e. the yield reduction from a disease-free attainable yield; and Ya is the
231 attainable yield, i.e., the yield level in the absence of disease. At the end of each crop growth phase, yield loss is
232 reset to zero, so that the new cropping cycle starts without losses.

233

234

235

236 2.3 Model parameters and initial values

237 Initial values are zero for all state variables (i , S , and YL). Parameters dimensions and values are listed in Table 1.
238 The durations of the crop establishment period (CEP) and of the crop growth period (CGP) are both set to 120
239 days, representing, for example, approximate durations for a winter wheat crop grown in a temperate region of
240 the world. An epidemic of the local strain is initiated at the end of CEP in the first cropping cycle with an initial
241 value ($starter$; Table 1) for the local strain of 0.01 day^{-1} . The conversion of surviving propagules into a rate of
242 primary infections ($convSP$) is set to 0.01, meaning that for example 100 surviving entities are translated into 1
243 primary infection during the first time step of CGP . The carrying capacity for injury level, $imax$, is set to 100 in
244 order to generate injury levels expressed as percent. In the same way, Ya , the attainable yield, is set to 100 in
245 order to generate yield losses expressed as percent.

246 RRL is set to 0.05, meaning that combined disease injury ($i_1 + i_2$), when at low levels, entails an increase
247 in yield loss at each time step which corresponds to 5% of the level of disease injury. RRg_1 and RRD_1 values are
248 set to 0.07 and 0.01, respectively.

249

250 2.4 Model analyses: conditions of emergence of an immigrant strain

251 2.4.1 Framework of analyses

252 We consider a pathosystem with two pathogen strains: a local (resident), and an immigrant (exogenous) strain.
253 The fitness of each of the two strains is represented by two essential components: the ability to reproduce
254 during the growing season [represented by a relative, or intrinsic, rate of growth, RRg_j in Equation (2)] and the
255 rate of population decay [represented by a relative, or intrinsic, rate of decay, RRD_j in Equation (3), Table 1], the
256 latter characterizing the ability of a pathogen strain to survive in the absence of host plants. As a convention,
257 the subscript $j=1$ refers to a local strain and $j=2$ refers to an immigrant strain. Fitter strains reproduce faster on
258 the host during the growing season and decay more slowly over time.

259 We addressed the question of emergence of immigrant strains as follows. A given agroecosystem
260 harbours a resident diversity of strains; however, all these strains are assumed to be equally adapted to the

261 considered agroecosystem – i.e. they have similar fitness. As a simplification, the entire population of resident
262 strains in an agroecosystem is therefore represented by one strain, exhibiting two central values for RRg_1 and
263 RRD_1 . Because these local populations are assumed to be established and in a dynamic equilibrium, we further
264 assume no variation over time for parameters RRg_1 and RRD_1 . In the absence of immigration, successive
265 epidemics occur in the considered agroecosystem. These epidemics consist of overlapping disease cycles
266 (polycyclic epidemics), and each epidemic results from the carry-over of inoculum from a previous epidemic
267 that took place in the previous crop seasons. The resulting pattern of disease over successive crop seasons
268 (polyetic process) in an agroecosystem thus results from the concatenation of successive (polycyclic) epidemics.

269 In order to investigate conditions for emergence, we consider an immigrant strain, which originates
270 from a very large pool of possible strains. In a first (deterministic) regime, the fitness parameters of the
271 immigrant strain, RRg_2 and RRD_2 , are assumed to be constant throughout the successive simulated cropping
272 seasons. In a second (stochastic) regime, the fitness parameters of the immigrant strain are drawn at random
273 from a normal distribution with central values RRg_2 and RRD_2 , and with variation about these values. This
274 drawing is made at the beginning of each cropping cycle, and the values drawn are kept constant within each
275 cropping cycle. This stochastic regime reflects the hypothesis of a strain which is not well adapted to the local
276 environment, with a fitness that varies as environmental conditions vary over cropping cycles.

277 The execution of the model over a succession of 30 cropping cycles is referred to as a simulation. We
278 investigated a scenario in which the immigrant strain is introduced once, at cropping cycle 10, at the beginning
279 of the growing season. This way, the immigrant strain is introduced into a stabilized system where the local
280 strain is already established. We used the simulation model (Section 2.2, Figure 2) to study two dynamic
281 regimes: (i) a deterministic regime, in which RRg_2 and RRD_2 had fixed values during a given simulation (section
282 2.4.2 below), and (ii) a stochastic regime, in which the values of either RRg_2 or RRD_2 or both were drawn from a
283 normal (Gaussian) distribution at the beginning of each cropping cycle and kept at these values during each
284 cropping cycle (section 2.4.3 below). We also derived approximate analytical expressions for the thresholds of

285 emergence of the immigrant strain by representing the simulation model as a discrete time map and
286 investigating its linear stability (Section 2.4.4 below and Appendix A).

287 The outcomes of the analyses were synthesised according to three features characterising disease
288 emergence of an immigrant strain and its consequences: the probability of emergence, the time to emergence,
289 and the yield loss associated with the emergence. We consider that the immigrant strain has emerged if it
290 exceeds the resident strain in terms of its AUDPC (area under disease progress curve, i.e., the accumulated
291 injury incurred within a growing season) during at least three cropping cycles after its introduction. The
292 probability of emergence, P_{emerg} , was estimated as the proportion of simulations that resulted in emergence. In
293 each individual simulation that resulted in emergence, the time to emergence, T_{emerg} , was defined as the
294 number of cropping cycles between the introduction of the immigrant strain and the first cropping cycle when
295 the AUDPC of the immigrant strain exceeded that of the resident strain. To quantify yield loss in each
296 simulation, we calculated the average yield losses caused by both the resident and the immigrant pathogen
297 strains over the 30 cropping cycles.

298 The model was developed using the Stella software (STELLA Architect version 1.1.2) and subsequently
299 translated to the Python programming language (version 3.4.3), where the bulk of the analysis was conducted.
300 The system of Equations (1)-(4) was solved and analysed using Python packages numpy (version 1.13.3) and
301 scipy (version 1.0.0), and the figures were produced using the Python package matplotlib (version 2.1.1). Parts
302 of the analytical investigation were performed with Wolfram Mathematica (version 10.3 for Linux).

303

304 2.4.2. Deterministic approach

305 We performed three sets of simulations in order to analyse the individual effects of RRg_2 , RRD_2 , and the
306 combined effects of RRg_2 and RRD_2 on disease emergence.

307 A first analysis was conducted to address conditions of emergence associated to RRg_2 . In this first
308 analysis, 100 simulations were run with RRg_2 increasing from 0.06 to 0.12 day⁻¹ with a constant increment of

309 RRg_2 between simulations, while RRD_2 was fixed (0.02 day^{-1}). The RRD_2 value chosen corresponds to the
310 hypothesis of an immigrant strain with a lower survival capacity than the resident strain ($RRD_1 = 0.01 \text{ day}^{-1}$). In
311 the second analysis, we assessed conditions of emergence according to RRD_2 . Here, 100 simulations were run
312 with RRD_2 increasing from 0 to 0.05 day^{-1} with a constant increment between simulations, while RRg_2 was fixed
313 (0.1 day^{-1}). This RRg_2 value corresponds to the hypothesis of an immigrant strain with a higher aggressiveness
314 than the resident strain ($RRg_1 = 0.07 \text{ day}^{-1}$). In a third analysis, both RRg_2 and RRD_2 were considered with respect
315 to emergence. RRg_2 and RRD_2 were varied in the same ranges as in the first and second analyses over a total of
316 10^4 simulations (100 x 100 runs).

317

318 2.4.3. Stochastic approach

319 As in the deterministic approach, the individual effects of RRg_2 , RRD_2 , and combined effects of RRg_2 and RRD_2
320 were subsequently analysed.

321 To address conditions of emergence associated to RRg_2 , 100 sets of simulations were executed with
322 fixed RRg_2 values ranging from 0.06 to 0.12 day^{-1} , with a constant increment. For each RRg_2 value considered
323 (i.e., for each set of simulations), 5000 stochastic runs were executed, within which the values of RRD_2 were
324 drawn at the beginning of each cropping cycle as random numbers from the normal (Gaussian) distribution with
325 the mean 0.02 day^{-1} and the standard deviation 0.007 day^{-1} . These RRD_2 values then remained constant during
326 the whole cropping cycle until the beginning of the next growing season, when a new random value was
327 chosen.

328 The second analysis was conducted in the same way as the first analysis, but focused on RRD_2 : 100 sets
329 of simulations were executed with fixed RRD_2 values ranging from 0 to 0.05 day^{-1} , with a constant increment.
330 For each RRD_2 value considered, 5000 stochastic runs were executed, within which the values of RRg_2 were
331 drawn at the beginning of each cropping cycle as random numbers from the normal distribution with mean 0.1

332 day⁻¹ and standard deviation 0.035 day⁻¹. These RRg_2 values then remained constant during the whole cropping
333 cycle.

334 In a third analysis, the values of both RRg_2 and RRD_2 were drawn from the normal distribution at the
335 beginning of each cropping cycle with means ranging from 0.05 to 0.12 day⁻¹ for RRG_2 , and ranging from 0 to
336 0.04 for RRD_2 , and with standard deviations constituting a constant proportion, 0.35, of the corresponding
337 mean values. As in the previous analyses, RRg_1 and RRD_1 values remained constant within each cropping cycle.
338 We ran 200 stochastic realizations for each point of the 100x100 grid of $RRg_2 \times RRD_2$ values considered.

339

340 2.4.4. Analytical approach

341 The overall fitness of the pathogen strain j is given by its polyetic (or multi-season) basic reproductive number
342 (see Appendix A for the derivation):

$$343 R_{op,j} = convSP \times \exp[(RRg_j \times T_s) - (RRD_j \times T_{BS})] \quad (5)$$

344 where T_s is the crop growth duration ($T_s = CGP$) and T_{BS} is the delay between two successive growing seasons.

345 The index "p" in R_{op} refers to "polyetic", in order to distinguish R_{op} from R_0 , which usually refers to the "within
346 season" basic reproductive number in the epidemiological literature (e.g., Zadoks and Schein, 1979; Anderson
347 and May, 1986; Campbell and Madden, 1990). Biologically, $R_{op,j}$ represents the number of units of crop injury
348 appearing at the beginning of a given growing season following the introduction of a unit host injury in the
349 beginning of the previous growing season. $R_{op,j}$ incorporates both the ability of a strain j to multiply during crop
350 growth and to survive between growing seasons. Hence, in the exponent of Eq. (5), the two components of
351 pathogen fitness, RRg_j and RRD_j , are weighted by T_s and T_{BS} , respectively.

352 As in the previous analysis, we consider the situation when the local pathogen strain is viable when
353 present alone: its reproduction during the growing season exceeds its losses between growing seasons, i.e.,
354 $R_{op,1} > 1$. In this case, the immigrant strain will emerge if its polyetic basic reproductive number exceeds the
355 polyetic basic reproductive number of the local strain, i.e., $R_{op,2} > R_{op,1}$. The emergence threshold corresponds to

356 $R_{0p,2} = R_{0p,1}$. We solve this equation with respect to RRg_2 and obtain the threshold value of RRg_2 above which
357 emergence takes place:

$$358 \quad RRg_{2,thresh} = [(T_{BS} / T_S) \times (RRD_2 - RRD_1)] + RRg_1. \quad (6)$$

359 Similarly, the emergence threshold can be expressed in terms of RRD_2 :

$$360 \quad RRD_{2,thresh} = [(T_S / T_{BS}) \times (RRg_2 - RRg_1)] + RRD_1. \quad (7)$$

361 Here, the immigrant strain emerges when its relative rate of decay is below the threshold, i.e., $RRD_2 < RRD_{2,thresh}$.

362 Eqs. (6) and (7) were derived under the assumption that the saturation effects of the logistic growth are

363 negligible. This is justified at sufficiently low relative rates of growth for each of the strains RRg_j , and at short

364 enough CGP, so that the host tissue does not become a limiting factor for any of the two pathogen strains. Note

365 that the simulation model in Sec. 2.2 does not make this approximation. See Appendix A for more mathematical

366 details.

367

368 **3. RESULTS**

369 3.1 An example of dynamics of crop injuries and losses simulated with the stochastic approach

370 Figure 3 displays examples of simulated dynamics using fitness parameters for the immigrant strain drawn from

371 a normal distribution at the beginning of each cropping cycle, the parameter values remaining fixed within a

372 given cropping cycle. Means of RRg_2 and RRD_2 are equal to the values used for the local strain (0.07 for RRg and

373 0.01 for RRD) and their standard deviations are 0.03 and 0.003, respectively. The three top panels display injury

374 dynamics leading to (1) non-emergence of the immigrant strain (Fig. 3a), (2) co-occurrence of both strains

375 where the predominant strain varies over cropping cycles (Fig. 3b), and (3) rapid emergence of the immigrant

376 strain (Fig. 3c). Because parameters are fixed for the local strain, simulation leading to non-emergence (Fig. 3a)

377 shows an equilibrium state with a maximum level of injury which reaches a constant value starting from the 6th

378 cropping cycle. When both strains co-exist (Fig. 3b), the stochasticity of RRg_2 and RRD_2 produces a large

379 variation over cropping cycles in both injury level and the respective frequency of each strain. In the case of

380 rapid emergence of the immigrant strain (Fig. 3c), the immigrant strain very quickly overcomes the local strain,
381 but displays a large variation in disease intensity over cropping cycles, because of stochasticity in RRg_2 and
382 RRD_2 .

383 Simulated yield loss, primary inoculum, and relative rates of growth and decay corresponding to the
384 example of a rapidly emerging strain (Fig. 3c) are displayed in Figure 3d-f. Yield losses vary over time (Fig. 3d),
385 with a pattern similar to that observed for injury dynamics (Fig. 3c). At the end of each crop season, the
386 terminal disease injury from each strain is proportionally converted to surviving propagules. The number of
387 surviving propagules then decays exponentially over time and constitutes the primary inoculum for the
388 subsequent growing season (Fig. 3e). This primary inoculum translates into primary infections at the beginning
389 of each crop growth phase (Fig. 3e). Relative rates of growth and of decay of the immigrant strain vary over
390 cropping cycles, while remaining constant within each cropping cycle (Fig. 3e). These stochastic values of RRg_2
391 and RRD_2 are driving the dynamics of injury (Fig. 3c) and of primary inoculum (Fig. 3e) over cropping cycles.

392

393 3.2 Individual effects of the relative rates of epidemic growth and inoculum decay on disease emergence

394 When we consider RRg_2 variation in the deterministic regime, P_{emerg} rises suddenly from zero to one as the RRg_2
395 value is increased (Fig. 4a, blue curve). The reason is that the immigrant strain can only emerge if it is able to
396 grow fast enough during the growing season. More fit immigrants, when they emerge (i.e., when $P_{\text{emerg}} = 1$ in
397 Fig. 4a), emerge more rapidly as RRg_2 increases: T_{emerg} decreases monotonically as we increase the immigrant
398 strain's fitness by increasing RRg_2 (Fig. 4c, blue curve). As we increase RRg_2 , the amount of disease caused by
399 the immigrant strain increases and so does the average yield losses incurred by both the resident and the
400 immigrant pathogen strains (Fig. 4e, blue curve). Below the emergence threshold (Fig. 4a, RRg_2 values for which
401 $P_{\text{emerg}} = 0$), the immigrant strain is absent, therefore the yield losses are only incurred by the resident strain, and
402 are not affected by RRg_2 . The analytical approach yields a threshold for emergence of RRg_2 at 0.09 day^{-1} (Fig. 4a,

403 grey line), that is, slightly smaller than the threshold derived from the deterministic approach (Fig. 4a, blue
404 line).

405 When we include stochasticity, the transition between parameter areas of “no emergence” and
406 “emergence” is now gradual: P_{emerg} increases continuously as RRg_2 values of the immigrant strain are increased
407 (red curve in Fig. 4a). Time to emergence also exhibits a different pattern in the stochastic regime. Emergence
408 starts at RRg_2 values much smaller than in the deterministic regime (Fig. 4c, red curve) with relatively small
409 values of T_{emerg} (about 2 cropping cycles), then T_{emerg} increases gradually, plateaus at about four cropping cycles,
410 and then declines with a curve close to, but above, that generated from the deterministic approach. Yield losses
411 show a similar pattern in the deterministic and stochastic regimes (compare red and blue curves in Fig. 4e),
412 although yield losses are somewhat lower in the stochastic regime than in the deterministic regime.

413 The effect of RRD_2 on emergence characteristics (Fig. 4b, d, f) mirrors the effect of RRg_2 (Fig. 4a, c, e),
414 because as fitness of the immigrant strain increases with RRg_2 , it decreases with RRD_2 . Under the deterministic
415 regime, P_{emerg} drops abruptly from one to zero as RRD_2 is increased (Fig. 4b, blue curve): the immigrant strain
416 cannot emerge if its population decays too fast between growing seasons. In the same way, less fit immigrants
417 emerge more slowly, when they do emerge: T_{emerg} increases monotonically as we reduce the immigrant strain's
418 fitness as RRD_2 increases (Fig. 4d, blue line). Average yield losses decrease as RRD_2 increases (Fig. 4f), and
419 remain stable when RRD_2 values are above the threshold for emergence. The threshold for emergence
420 generated from the analytical approach, $RRD_2 = 0.025$, is slightly lower than the threshold generated from the
421 deterministic approach (Fig. 4b).

422 When we include stochasticity, P_{emerg} diminishes continuously as RRD_2 is increased; time to emergence,
423 T_{emerg} , increases initially (with values slightly larger than those obtained from the deterministic approach),
424 reaches a maximum around the emergence threshold and gradually declines to small values. Yield losses show
425 a qualitatively similar pattern in the deterministic and stochastic regimes. As when investigating the effect of
426 RRg_2 , yield losses are lower in the stochastic regime than in the deterministic regime (Fig. 4f).

427

428 3.3 Combined effects of the relative rates of epidemic growth and inoculum decay on disease emergence

429 When using the deterministic approach, emergence and no emergence domains are clearly separated by a

430 straight line (Fig. 5a). This line reflects the abrupt transition from emergence to no emergence, as illustrated in

431 Figs. 4a and 4d. The domain of emergence corresponds to pairs of values of RRg_2 and RRD_2 below which

432 emergence takes place: for a given value of RRg_2 , emergence will occur within a range of values of RRD_2 below a

433 given threshold. The dashed lines in Fig. 5a display the outcomes for fitness values used which correspond to

434 that of the resident strain. At $RRg_2 = RRg_1 = 0.07$, emergence occurs for RRD_2 values slightly smaller than RRD_1 .

435 Similarly, at $RRD_2 = RRD_1 = 0.01$, emergence occurs for RRg_2 values that are slightly larger than RRg_1 . The solid

436 grey line represents the analytical expression for the emergence threshold in terms of RRD_2 , according to

437 Equation (7). That is, a line with slope (T_s / T_{BS}) which equals 0.5 in our case, and an ordinate at origin of -0.025.

438 When stochasticity is included in the model, the transition between parameter domains of emergence

439 and no emergence becomes gradual (Fig. 5b). This gradual transition is a generalisation of the gradual change in

440 emergence probability according to RRg_2 and RRD_2 illustrated in Figs. 4a and 4d, respectively. As in Fig. 5a, the

441 dashed black line represents the fitness parameters of the resident strain. In the same way, the parameter

442 region explored in Fig. 4a and 4b is materialised with the yellow lines which refer to $RRg_2 = 0.1$ and $RRD_2 = 0.02$.

443 The most important effect of stochasticity is that emergence occurs at ranges of parameters that are below the

444 emergence threshold, where no emergence was possible according to the deterministic approach (within the

445 white area in Fig. 5a). Even if the immigrant strain is on average less fit than the local strain (i.e., in terms of its

446 average fitness components $RRg_2 < RRg_1$, $RRD_2 > RRD_1$), there is still a non-zero probability for its emergence.

447 This scenario corresponds to the region in Fig. 5b above the black horizontal line and to the left from the black

448 vertical line.

449

450

451 **4. DISCUSSION**

452 4.1 Key findings

453 The modelling framework which was designed in this work enables analysing the conditions underlying disease
454 emergence. According to our pre-set specifications, the model includes polyetism, stochasticity, and yield loss.
455 The analyses conducted here allow identifying important features associated with disease emergence.

456 A major finding is that stochasticity can be an important boundary condition for disease emergence.
457 Emergence reflects important changes in the status of a system (here crop health) that can be caused by rare
458 events (e.g., Paini *et al.*, 2016), associated with small sizes of immigrant or mutant subpopulations that initiate
459 the process, and by polyetic processes that lead to significant reductions in population size between growing
460 seasons (Shaw, 1994). Stochasticity associated with genetic factors such as bottlenecks and genetic drift is
461 known to play an important role in the evolution of a host-pathogen interaction (McDonald, 2004).
462 Stochasticity can also be introduced by environmental factors such as climatic conditions, which can
463 differentially affect the fitness of strains in pathogen populations (e.g., Gilligan and Van den Bosch, 2008). In the
464 present study, we focused on the latter, environmentally-induced, stochasticity.

465 Previous modelling analyses considered polyetic processes (e.g., Gubbins *et al.*, 2000; Madden and Van
466 den Bosch, 2002) under a deterministic framework, leading to identification of thresholds for persistence.
467 Results generated from the stochastic approach in this work produce a different outcome, in showing that (1)
468 even when an immigrant strain is drawn from a population which is, on average, less fit than the local strain,
469 the immigrant strain may nevertheless emerge due to stochasticity; and conversely (2) even when an immigrant
470 strain is drawn from a population which is, on average, more fit than the local strain, the immigrant strain will
471 not necessarily emerge, and may face extinction. An important implication of this finding is that emergence
472 may require a series of independent immigration events involving new pathogen strains before a successful
473 invasion takes place. In some cases, a pathogen that appears to have suddenly emerged over the course of only
474 1-2 cropping cycles may have been present at a low level for decades before the proper conditions (e.g.

475 conducive weather conditions) occurred to enable an explosion in population size and an observed
476 "emergence". This has important implications to guide future research, both in terms of modelling and
477 experimentation, and potentially to inform policy on emerging diseases.

478 Another important finding from our analyses is that survival between growing seasons is as important
479 for emergence as the pathogen reproduction during the growing season. Pathogens with limited saprophytic
480 abilities and lacking durable survival structures such as chlamydospores, sclerotia or oospores are expected to
481 undergo large bottlenecks between host growing seasons that will purge genetic diversity and increase the
482 probability that less well-adapted immigrants occurring at lower frequencies will go extinct between growing
483 seasons. Conversely, pathogens that compete well as saprophytes and/or produce long-lived survival structures
484 will maintain high effective population sizes that sustain high levels of genetic diversity across growing seasons,
485 enabling persistence of immigrants and novel mutants for long periods of time, even if they are less well
486 adapted, and increasing the probability that these immigrants, mutants or recombinants can make a successful
487 invasion. Although the importance of the survival phase has been recognized in earlier work (e.g., Heesterbeek
488 and Zadoks, 1987; Gubbins *et al.*, 2000; Madden and Van den Bosch, 2002, Hamelin *et al.*, 2011), survival has
489 often been overlooked by plant pathologists. Conversely, RRg can be seen as the apparent infection rate of Van
490 der Plank (r_L ; Campbell and Madden, 1990), for which ranges have been measured from disease progress curves
491 in many instances. The RRg ranges explored in our analyses (0.05 to 0.12) fit well within ranges measured for
492 epidemics of annual crop diseases (Kranz, 2003).

493
494 4.2 Comparing outcomes from the deterministic, analytical, and stochastic approaches

495 There is a good agreement between the analytical emergence thresholds (Eq. (6) and (7)) and the numerical
496 thresholds in the deterministic regime, although the threshold for emergence with respect to RRg is slightly
497 lower when derived from the analytical approach as compared to the deterministic approach (Figs. 4, 5a), while
498 the opposite pattern is obtained for RRD (Figs. 4b, 5a). This difference can be explained by the limited duration

499 (30 cropping cycles) of the numerical simulations. In some cases, the immigrant strain would be able to emerge,
500 but this would require more than 30 cropping cycles. On the contrary, the analytical threshold does not restrict
501 the number of cropping cycles and therefore generates thresholds for emergence that can occur over an infinite
502 time span. This explanation was confirmed by performing additional simulations conducted using the same
503 design that generated Figure 4, but including many additional cropping cycles (200). In that case, the agreement
504 between the two thresholds (from deterministic simulations and from analytical expressions) was perfect. In
505 future analyses using this framework, the threshold values to consider (from deterministic or analytical
506 approaches) will depend on the modelling objectives and the applications under consideration.

507 When investigating the probability of emergence, fitness thresholds are derived from the deterministic
508 approach, while such thresholds do not materialize in the stochastic approach because the emergence
509 probability can take values between 0 and 1. The stochastic approach allows a strain with a fitness (RRg or RRD)
510 mean value below the deterministic emergence threshold (i.e., lower values for RRg and larger values for RRD)
511 to emerge, with a probability which progressively declines as the mean fitness value moves away from the
512 threshold.

513 The time to emergence progressively declines as the fitness values increase in the deterministic
514 approach because it requires progressively less time for the immigrant strain to outcompete the resident strain.
515 Under the stochastic regime, a different pattern is exhibited, with the time for emergence increasing, reaching a
516 maximum, and eventually declining as the fitness values increase. This pattern can be interpreted as follows: at
517 low average fitness, the only way to achieve emergence in the stochastic regime is when high fitness values
518 from the tail of the distribution are drawn over several consecutive growing seasons, representing particularly
519 "lucky" realizations. There is a small proportion of such realizations (reflected by the small probability of
520 emergence), as they correspond to quite rare events, but when they do happen, emergence occurs relatively
521 fast. In contrast, at higher average fitness, there can be many other paths to emergence including those
522 realizations in which high fitness values appear sporadically, not necessarily in several consecutive seasons,

523 leading to slower emergence on average. Thus, the two competing effects, (i) longer emergence due to reduced
524 mean fitness of the immigrant strain in the range of high fitness values and (ii) the preferential emergence of
525 only "lucky", "fast-emerging" realizations in the range of low fitness values, lead to emergence time reaching a
526 maximum in the stochastic regime.

527 Yield losses derived from the stochastic regime are lower than yield losses derived from the
528 deterministic approach (Figs. 4e, f). This difference can be seen as the consequence of differences observed
529 between these regimes both in terms of the probability of emergence (Figs. 4a, b) and the time to emergence
530 (Figs 4c, d): above the deterministic threshold, there are cases where disease does not emerge, or where time
531 to emergence is delayed in the stochastic approach, and therefore yield losses are not as high as in the
532 deterministic approach.

533

534 4.3 Further questions to address on disease emergence

535 Our analyses provide a series of elements to better understand how disease emerges. The model structure
536 allows addressing other important questions on disease emergence, such as:

537 - the effect of primary infection patterns on emergence: in the analyses we conducted, we considered only one
538 type of primary infection, as a single immigration event occurring at a single point in time. The model allows the
539 consideration of other patterns, including varying size of immigrant inoculum, or repeating inflows of immigrant
540 strains over several cropping seasons (instead of during only one cropping season).

541 - the immigration rate simply considers the entry into the system of a new strain, with no specific hypothesis
542 attached to the origin of this strain. The model also allows consideration of other potential sources of new
543 strains, including recombinants or mutants, which could originate from inside or outside of the zone of
544 emergence.

- 545 - the model can also include adaptation of the pathogen population, for example by varying RRg and RRD over
546 time, or draw new parameters at the start of each cropping cycle according to the parameter values of the
547 preceding cropping cycle (Figure 1, path 3).
- 548 - the effect of variation of RRg within the growing season can be analysed in order to mimic the effect of
549 weather (e.g. warmer winters or drier summers) on epidemics and emergence (Figure 1, Path 2).
- 550 - the analyses were conducted with a relatively limited number of cropping cycles of simulation. This was
551 appropriate because a large amount of inoculum was used in the simulations. When considering a low rate of
552 immigration within a stochastic regime, much longer time frames may be needed to detect emergence.
- 553 - the effect of climate change on disease emergence can be addressed with this model by incorporating a
554 directional change in the mean and/or the standard deviation of some fitness parameters (e.g., RRg and RRD)
555 over successive cropping cycles.

556

557 Plant disease emergence is a complex phenomenon, with many system- and context-specific variants.
558 This work addresses the phenomenon in a simplified manner in order to derive some of its main features.
559 While this work needs to be continued, we hope that the present analysis provides a useful step towards
560 implementing more effective policies to prevent or delay plant disease emergence.

561

562 **DATA AVAILABILITY STATEMENT**

563 The data that support the findings of this study are available from the corresponding author upon reasonable
564 request.

565 **REFERENCES**

- 566 Anderson, P. K., Cunningham, A.A., Patel, N.G., Morales, F.J., Epstein, P.R. and Daszak, P. (2004) Emerging
567 infectious diseases of plants: pathogen pollution, climate change and agrotechnology drivers. *Trends in*
568 *Ecology and Evolution*, 19, 535-544.
- 569 Anderson, R.M. and May, R.M. (1986) The invasion, persistence and spread of infectious diseases within animal
570 and plant communities. *Philosophical Transactions of the Royal Society of London B, Biological Sciences*, 314,
571 533-570.
- 572 Campbell, C.L. and Madden, L.V. (1990) *Introduction to Plant Disease Epidemiology*. New York, USA: John Wiley
573 and Sons.
- 574 Ceresini, P.C., Castroagudín, V.L., Rodrigues, F.Á., Rios, J.A., Aucique-Pérez, C.E., Moreira, S.I. *et al.* (2018) Wheat
575 blast: past, present, and future. *Annual Review of Phytopathology*, 56, 427-456.
- 576 Fisher, M.C., Henk, D.A., Briggs, C.J., Brownstein, J.S., Madoff, L.C., McCraw, S.L. and Gurr, S.J. (2012) Emerging
577 fungal threats to animal, plant and ecosystem health. *Nature*, 484, 186-194.
- 578 Forrester, J.W. (1961) *Industrial Dynamics*. Cambridge, Mass., USA: M.I.T. Press.
- 579 Gilligan, C.A. and Van den Bosch, F. (2008) Epidemiological models for invasion and persistence of pathogens.
580 *Annual Review of Phytopathology*, 46, 385-418.
- 581 Gilligan, C.A., Truscott, J.E. and Stacey, A.J. (2007) Impact of scale on the effectiveness of disease control
582 strategies for epidemics with cryptic infection in a dynamical landscape: an example for a crop disease.
583 *Journal of the Royal Society Interface*, 4, 925-934.
- 584 Goodwin, S.B., Sujkowski, L.S. and Fry, W.E. (1996) Widespread distribution and probable origin of resistance to
585 metalaxyl in clonal genotypes of *Phytophthora infestans* in the United States and western Canada.
586 *Phytopathology*, 86, 793-799.
- 587 Gottwald, T.R. (2010) Current Epidemiological Understanding of Citrus Huanglongbing. *Annual Review of*
588 *Phytopathology*, 48, 119-39.

- 589 Gubbins, S., Gilligan, C.A. and Kleczkowski, A. (2000) Population dynamics of plant–parasite interactions:
590 thresholds for invasion. *Theoretical Population Biology*, 57, 219-233.
- 591 Hamelin, F.M., Castel, M., Poggi, S. and D. and Mailleret, L. (2011) Seasonality and the evolutionary divergence
592 of plant parasites. *Ecology*, 92, 2159-2166.
- 593 Heesterbeek, J.A.P. and Zadoks, J. C. (1987) Modelling pandemics of quarantine pests and diseases: problems
594 and perspectives. *Crop Protection*, 6, 211-221.
- 595 Kranz, J. (2003) *Comparative Epidemiology of Plant Diseases*. Berlin, Germany: Springer.
- 596 Leonard, K.J. (1977) Selection pressures and plant pathogens. *Annals of the New York Academy of Sciences*, 287,
597 207-222.
- 598 Lucas, J.A. (2017) Fungi, food crops, and biosecurity: advances and challenges. In: *Advances in Food Security*
599 *and Sustainability*. Amsterdam, The Netherlands: Elsevier, pp. 1-40.
- 600 Madden, L.V., Van Den Bosch, F. (2002) A population-dynamics approach to assess the threat of plant pathogens
601 as biological weapons against annual Crops. *BioScience*, 52, 65-74.
- 602 McDonald, B.A. (2004) *Population Genetics of Plant Pathogens*. APSnet Education Center. The Plant Health
603 Instructor. doi:10.1094/PHI-A-2004-0524-01
- 604 McDonald, B.A., Stukenbrock, E. H. (2016) Rapid emergence of pathogens in agro-ecosystems: global threats to
605 agricultural sustainability and food security. *Philosophical Transactions of the Royal Society of London B,*
606 *Biological Sciences*, 371, 20160026.
- 607 McMullen, M., Bergstrom, G., De Wolf, E., Dill-Macky, R., Hershman, D., Shaner, G. and Van Sanford, D. (2012) A
608 unified effort to fight an enemy of wheat and barley: Fusarium head blight. *Plant Disease*, 96, 1712-1728.
- 609 Paini, D.R., Sheppard, A.W., Cook, D.C., De Barro, P.J., Worner, S.P. and Thomas, M.B. (2016) Global threat to
610 agriculture from invasive species. *Proceedings of the National Academy of Sciences*, 113, 7575-7579.
- 611 Roelfs, A.P. (1978) *Estimated losses caused by rust in small grain cereals in the United States—1918–76*. US
612 Department of Agriculture, Miscellaneous Publications, 1363, 85 pp.

- 613 Roelfs, A.P. (1985) Wheat and Rye stem rust. In: Roelfs, A.P. Bushnell, W.R. (Eds.), *The Cereal Rusts. Volume II:*
614 *Diseases Distribution, Epidemiology, and Control*. Orlando, USA: Academic Press.
- 615 Saponari, M., Giampetruzzi, A., Loconsole, G., Boscia and D., Saldarelli, P. (2019) *Xylella fastidiosa* in olive in
616 Apulia: where we stand. *Phytopathology*, 109, 175-186.
- 617 Savary, S. and Willocquet, L. (2014) *Simulation Modeling in Botanical Epidemiology and Crop Loss analysis*.
618 APSnet Education Center. The Plant Health Instructor. doi: 10.1094/PHI-A-2014-0314-01.
- 619 Savary, S., Begaglio, S., Willocquet, L., Gustafson, D., Mason, D'Croz D., Sparks, A., et al. (2017) Crop health and
620 its global impacts on the components of food security. *Food Security*, 9, 311-327.
- 621 Savary, S., Willocquet, L., Pethybridge, S.J., Esker, P., McRoberts, N. and Nelson, A. (2019) The global burden of
622 pathogens and pests on major food crops. *Nature Ecology & Evolution*, 3, 430-439.
- 623 Savary, S., Teng, P.S., Willocquet, L. and Nutter, F.W. Jr. (2006) Quantification and modeling of crop losses: a
624 review of purposes. *Annual Review of Phytopathology*, 44, 89-112.
- 625 Saunders, D.G., Pretorius, Z.A. and Hovmøller, M.S. (2019) Tackling the re-emergence of wheat stem rust in
626 Western Europe. *Communications Biology*, 2, 51.
- 627 Shaw, M.W. (1994) Seasonally induced chaotic dynamics and their implications in models of plant disease. *Plant*
628 *Pathology*, 43, 790-801.
- 629 Singh, R. P., Hodson, D.P., Jin, Y., Lagudah, E.S., Ayliffe, M.A., Bhavani, S., et al. (2015) Emergence and spread of
630 new races of wheat stem rust fungus: continued threat to food security and prospects of genetic control.
631 *Phytopathology*, 105, 872-884.
- 632 de Vallavieille-Pope, C., Bahri, B., Leconte, M., Zurfluh, O., Belaid, Y., Maghrebi, E., et al. (2018) Thermal
633 generalist behaviour of invasive *Puccinia striiformis* f. sp. *tritici* strains under current and future climate
634 conditions. *Plant Pathology*, 67, 1307-1320.
- 635 Van den Berg, F., Bacaer, N., Metz, J.A., Lannou, C. and van den Bosch, F. (2011) Periodic host absence can select
636 for higher or lower parasite transmission rates. *Evolution Ecology*, 25, 121-137.

- 637 Wilcox, B.A. and Colwell, R.R. (2005) Emerging and reemerging infectious diseases: biocomplexity as an
638 interdisciplinary paradigm. *EcoHealth*, 2, 244-257.
- 639 Zadoks, J.C. (1974) The role of epidemiology in modern phytopathology. *Phytopathology* 64, 918-923.
- 640 Zadoks, J.C. and Schein, R.D. (1979) *Epidemiology and Plant Disease Management*. New York, USA: Oxford
641 University Press.
- 642 Zwankhuizen, M.J. and Zadoks, J.C. (2002) *Phytophthora infestans's* 10-year truce with Holland: a long-term
643 analysis of potato late-blight epidemics in the Netherlands. *Plant Pathology*, 51, 413-423.
- 644

645 **Appendix A**

646

647 Assuming that the dynamics of the two pathogen strains are independent of each other, the simulation model
648 described in Sec. 2.2 [Eqs. (1)-(4)] can be summarised in a single equation:

$$649 \quad i_{j,t+1} = R(i_{j,t})i_{j,t} \quad (\text{A1})$$

650 Where

$$651 \quad R(i_{j,t}) = \frac{imax \times convSP \times \exp[(RRg_j \times T_s) - (RRD_j \times T_{BS})]}{imax + i_{j,t} [\exp(RRg_j \times T_s) - 1]} \quad (\text{A2})$$

652 Here, $i_{j,t}$ is the injury caused by the pathogen strain j ($j=1$ for the local strain, and $j=2$ for the immigrant strain) at
653 the very beginning of the growing season t , where t is the index that runs through successive cropping cycles
654 (i.e., $t = 1, 2, 3, \dots$). T_s is the duration of the growing season (= CGP) and T_{BS} is the duration between two successive
655 growing seasons. Eq. (A1) is a map that relates the injury at the beginning of growing season $t+1$, $i_{j,t+1}$, to the
656 injury at the beginning of the previous growing season t , $i_{j,t}$, representing a nonlinear generalisation of the
657 classical geometric growth model. The map Eq. (A1) has two fixed points:

$$658 \quad i_{j,FP1} = 0; i_{j,FP2} = \frac{imax \times convSP \times \exp[(RRg_j \times T_s) - (RRD_j \times T_{BS})] - imax}{\exp(RRg_j \times T_s) - 1} \quad (\text{A3})$$

659 The fixed points determine the long-term outcomes of the dynamics: eventually the strain j either dies out
660 (FP1) or reaches the stable equilibrium (FP2). The equilibrium occurs due to a balance between pathogen
661 reproduction during the growing season and its decay between growing seasons: the number of newly
662 produced pathogen individuals during the growing season compensates the number of individuals lost during
663 the preceding between-growing season phase. Which of the two fixed points is achieved in the long run, is
664 determined by the growth rate of the map Eq. (A1) linearised in the vicinity of FP1:

$$665 \quad R_{op,j} = convSP \times \exp[(RRg_j \times T_s) - (RRD_j \times T_{BS})] \quad (\text{A4})$$

666 where $R_{0p,j}$ quantifies the reproductive fitness of the strain j and corresponds here to the polyetic basic
667 reproductive number. Usually, the basic reproductive number is defined as the number of host individuals that
668 are infected by a single infected host introduced into a fully susceptible host population (e.g., Zadoks and
669 Schein, 1979; Anderson and May, 1986; Campbell and Madden, 1990). Adapted to our context, the biological
670 meaning of $R_{0p,j}$ is the number of units of crop injury appearing at the beginning of growing season $t + 1$
671 following the introduction of a unit host injury at the beginning of the previous growing season t . If each of the
672 two strains is viable when present alone, i.e., $R_{0p,j} > 1$, the strain that has a higher basic reproductive number
673 eventually outcompetes the other strain. Consequently, the immigrant strain emerges if it has a higher polyetic
674 basic reproductive number, i.e., $R_{0p,2} > R_{0p,1}$. The emergence threshold is given by the equality of the two
675 polyetic basic reproductive numbers: $R_{0p,2} = R_{0p,1}$. We solve this equation with respect to RRg_2 , using Eq. (A4), to
676 obtain the threshold value of RRg_2 above which the emergence takes place:

$$677 \quad RRg_{2,thresh} = (T_{BS} / T_S) \times (RRd_2 - RRd_1) + RRg_1 \quad (A5)$$

678 Similarly, the emergence threshold can be expressed in terms of RRD_2 :

$$679 \quad RRD_{2,thresh} = (T_S / T_{BS}) \times (RRg_2 - RRg_1) + RRD_1 \quad (A6)$$

680 Here, the immigrant strain emerges when its relative decay rate is below the threshold, i.e., $RRD_2 < RRD_{2,thresh}$.
681 When only one pathogen strain is present, $R_{0p,j}$ given by Eq. (A4) determines without any approximation which
682 of the two fixed points in Eq. (A3) will be achieved according to the map in Eq. (A1). However, when both
683 pathogen strains are present, Eq. (A4) and Eqs. (A5), (A6) derived from it, give only approximate expressions for
684 emergence thresholds, under the assumption that the saturation effects of the logistic growth are negligible.
685 Nevertheless, $i_{j,FP2}$ in Eq. (A3) provides an exact expression for the final, equilibrium level of injury due to the
686 pathogen strain that wins the competition.

687

Table 1. Description of the model variables

Acronym	Definition	Dimension	Unit	Value
State variables:				
<i>i</i>	Injury caused by disease on a crop stand	[-]	%	0 to 100
<i>S</i>	Number of surviving propagules	[-]	%	0 to 100
<i>YL</i>	Yield loss – yield reduction from a disease-free attainable yield	[-]	%	0 to 100
Rates:				
<i>RPI</i>	Rate of primary infections	[T ⁻¹]	% Day ⁻¹	
<i>RconvIS</i>	Rate of conversion from injury (<i>i</i>) into surviving propagules (<i>S</i>)	[T ⁻¹]	% Day ⁻¹	
<i>Rdecay</i>	Rate of decay of surviving propagules	[T ⁻¹]	% Day ⁻¹	
<i>resetYL</i>	Rate of reset of yield loss at each cropping cycle	[T ⁻¹]	% Day ⁻¹	
<i>RI</i>	Rate of injury increase	[T ⁻¹]	% Day ⁻¹	
<i>RL</i>	Rate of yield loss	[T ⁻¹]	% Day ⁻¹	
<i>RM</i>	Rate of immigration of the pathogen	[T ⁻¹]	% Day ⁻¹	
<i>starter</i>	Rate of infection to initiate epidemics	[T ⁻¹]	% Day ⁻¹	
Parameters:				
<i>CEP</i>	Duration of the crop establishment period	[T]	Day	120
<i>CGP</i>	Duration of the crop growth period	[T]	Day	120
<i>convSP</i>	Conversion of surviving propagules into a rate of primary infections	[T ⁻¹]	Day ⁻¹	0.01
<i>imax</i>	Carrying capacity of injury – maximum level of injury	[-]	%	100
<i>RRD_j</i>	Relative rate of decay of surviving propagules for strain <i>j</i>	[T ⁻¹]	Day ⁻¹	<i>j</i> = 1: 0.01 <i>j</i> = 2: Varying
<i>RRg_j</i>	Relative rate of epidemic (injury) increase for strain <i>j</i>	[T ⁻¹]	Day ⁻¹	<i>j</i> = 1: 0.07 <i>j</i> = 2: Varying
<i>RRL</i>	Relative rate of yield loss	[T ⁻¹]	Day ⁻¹	0.05
<i>Ya</i>	Attainable yield – uninjured yield level	[-]	%	100

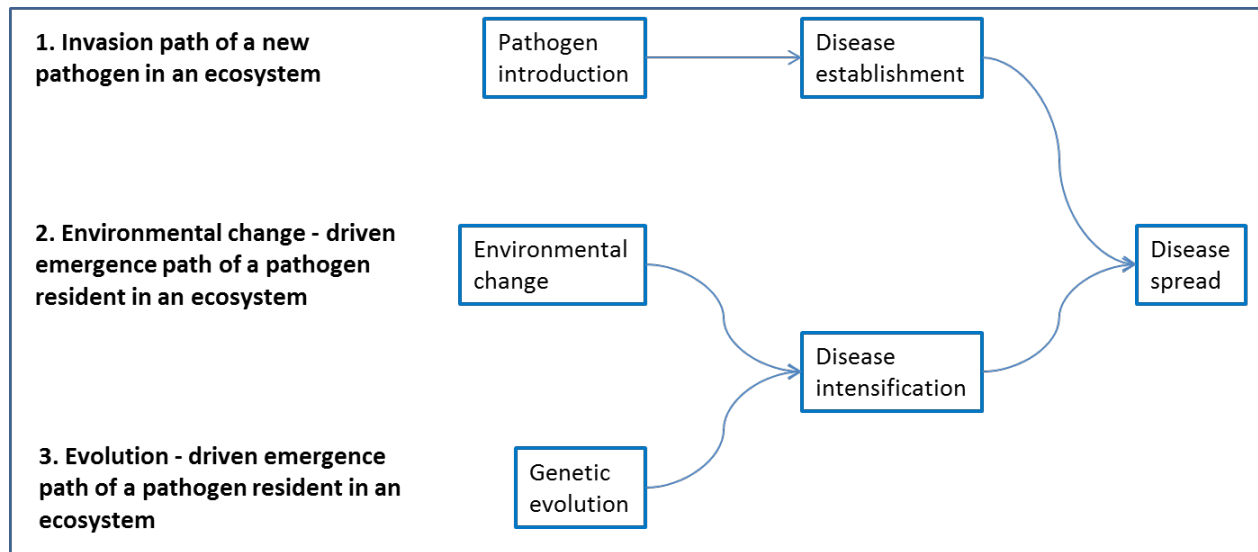


Fig. 1. A framework for analysis of emerging epidemics: paths and processes. Three paths for emergence are considered (left, bold characters), involving different processes (in boxes). Paths may be combined, e.g., paths 1 and 3, involving both introduction and evolution, or 2 and 3, involving environmental change and evolution. See text for examples.

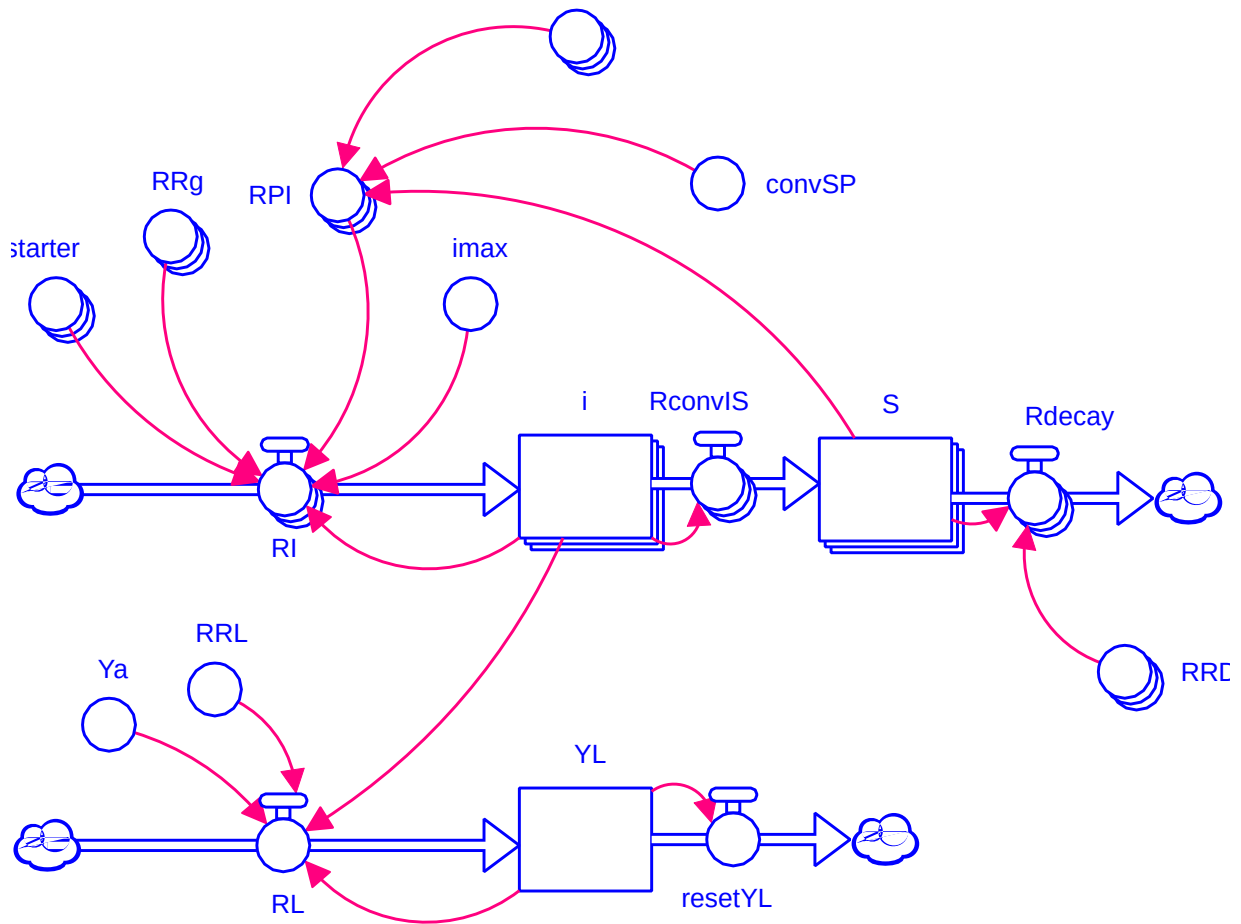


Fig. 2. Simplified flowchart of the process-based model used to analyse emerging diseases of crop plants. Variable acronyms are described in Table 1. The flowchart uses symbols introduced by J Forrester (Forrester, 1961): rectangles represent state variables; valves represent rates of change of state variables; circles represent parameters or computed variables. Stacked symbols (e.g., state variables) represent vectors of two pathogen strains.

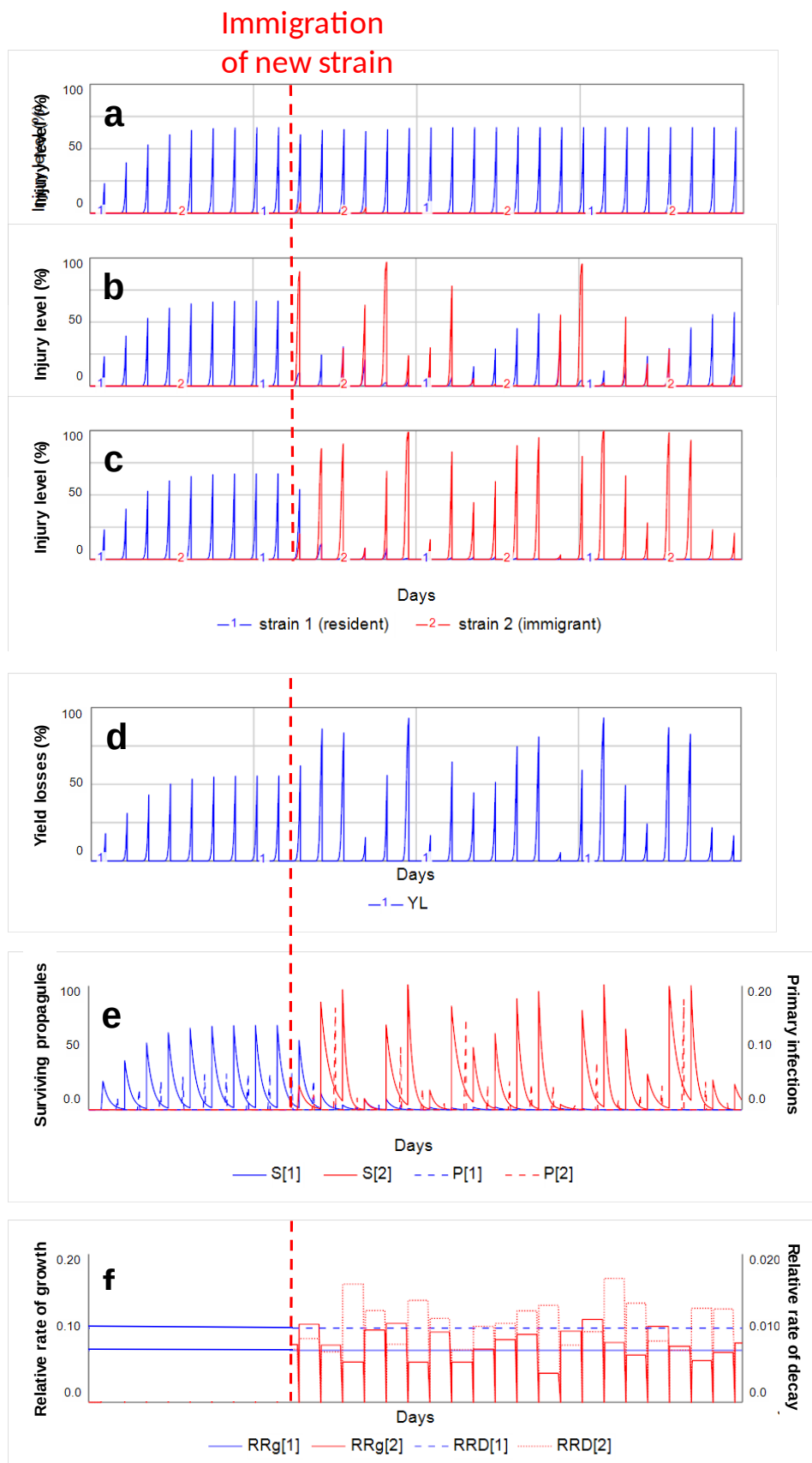


Fig. 3. Examples of simulated dynamics of injury levels and related variables over 30 cropping cycles.

(a) to (c): simulated injury levels from different runs where $RRg_2 \sim N(0.07, 0.03)$ and $RRD_2 \sim N(0.01, 0.003)$. (a): a simulation where the immigrant strain did not emerge; (b): a simulation where the immigrant and resident strains compete over cropping cycles; (c): a simulation where the immigrant strain replaces the resident strain; (d) to (f): simulated dynamics of other variables, associated with the dynamic of injury levels shown in (c).

Except for RRg_2 and RRD_2 , all parameters are set according to Table 1. Immigration of strain 2 takes place at the end of the crop establishment period of cropping cycle 10, while strain 1 is established at the beginning of the simulation.

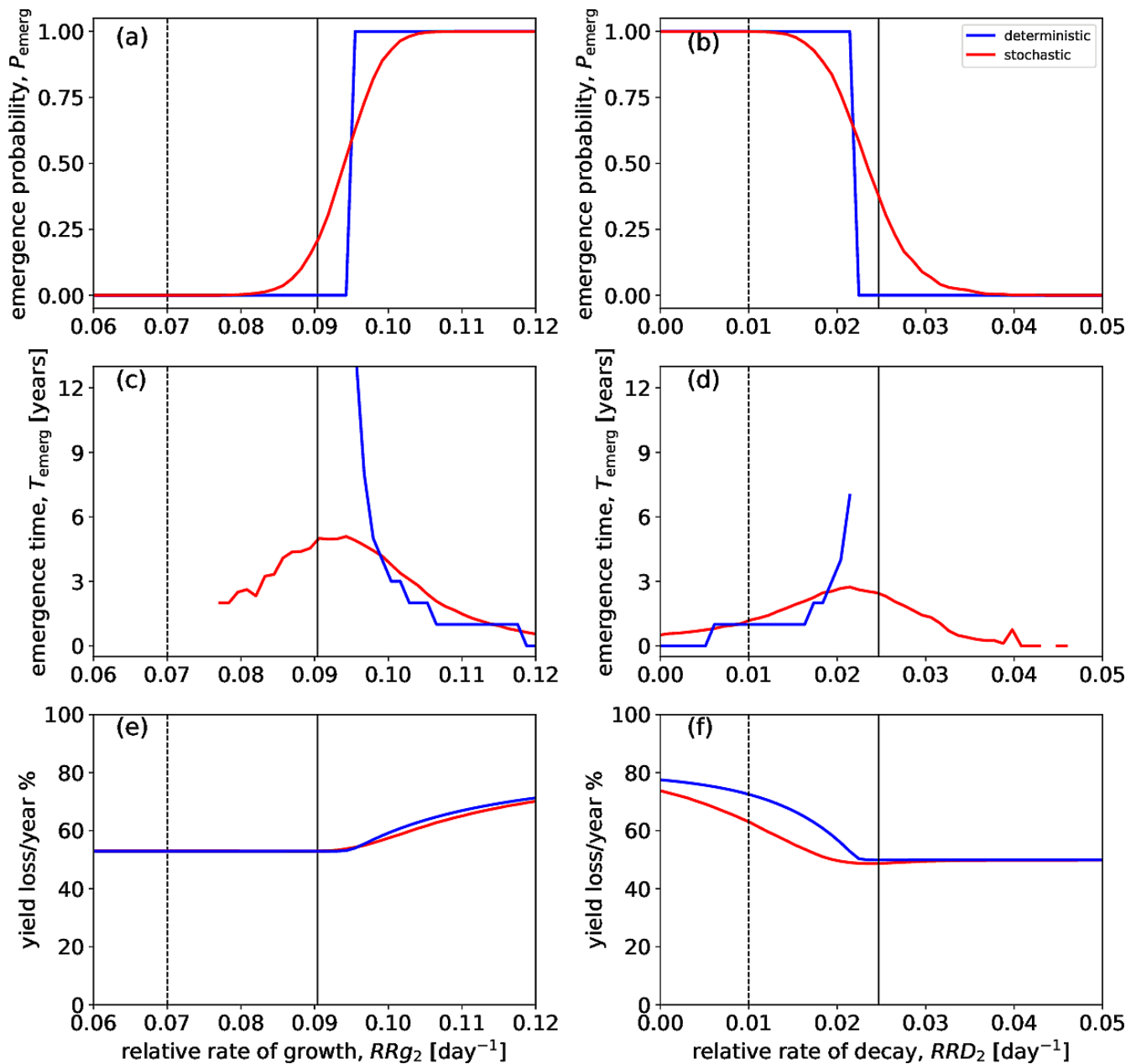


Fig. 4. Effects of pathogen reproduction and survival parameters on disease emergence and yield loss.

Emergence probabilities (a), (b), emergence times (c), (d) and yield losses (e), (f) are plotted versus the relative rate of growth, RRg_2 (a), (c), (e), and the relative rate of decay, RRD_2 (b), (d), (f), of the immigrant strain.

Blue curves correspond to the deterministic regime, in which both RRg_2 and RRD_2 have fixed, deterministic values, whereas red curves correspond to the stochastic regime. Red curves in panels (a), (c), (e) were

computed with the values of RRD_2 drawn as random numbers from the normal (Gaussian) distribution at the

beginning of each cropping cycle with the mean 0.02 day^{-1} and the standard deviation 0.007 day^{-1} , while RRg_2

assumed fixed, deterministic values. Similarly, red curves in panels (b), (d), (f) were computed with the values of RRg_2 drawn as random numbers from the normal (Gaussian) distribution at the beginning of each cropping cycle with the mean 0.1 day^{-1} and the standard deviation 0.035 day^{-1} , while RRD_2 assumed fixed, deterministic values.

Dashed vertical lines indicate the value of the relative rate of growth, $RRg_1=0.07$, of the resident strain in (a), (c), (e), and the value of the relative rate of decay, $RRD_1=0.01$, of the resident strain in (b), (d), (f). Solid vertical lines show the approximate analytical emergence thresholds, according to Eq. (6) in (a), (c), (e) and Eq. (7) in (b), (d), (f). Values of other parameters are given in Table 1.

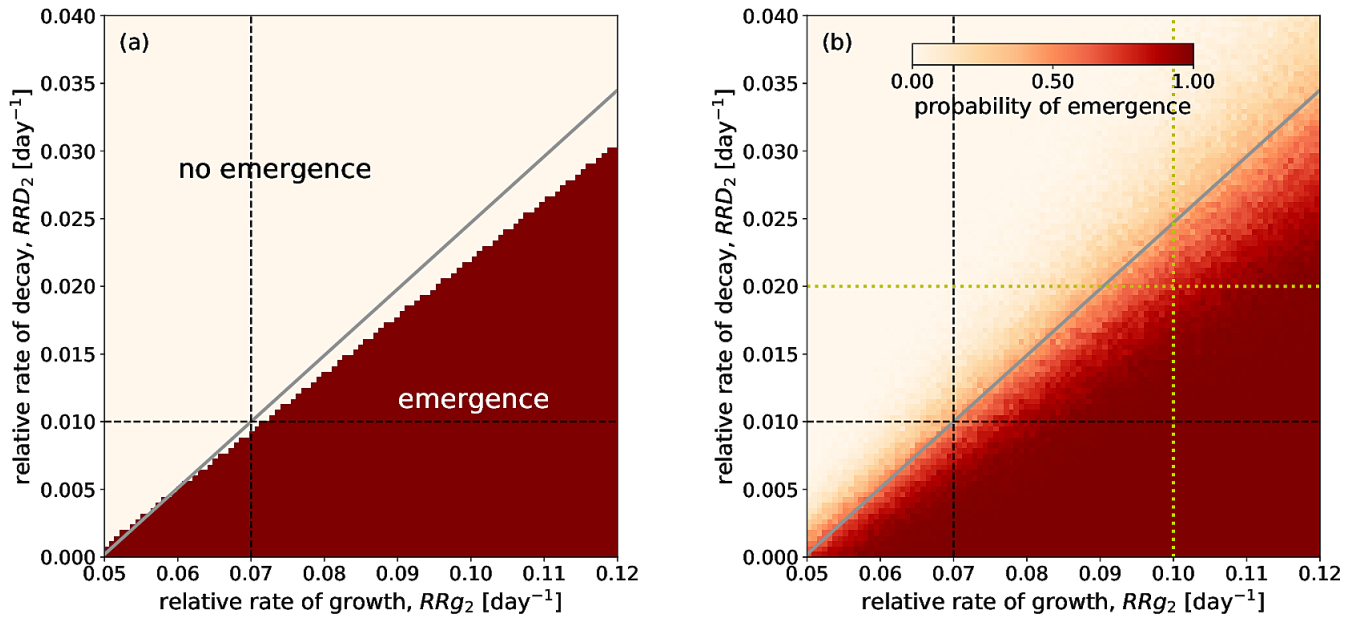


Fig. 5. Combined effects of pathogen reproduction and survival parameters on probability of emergence.

(a) deterministic regime; (b) stochastic regime, whereby the values of RRg_2 and RRD_2 were drawn from the normal (Gaussian) distribution at the beginning of each cropping cycle with the mean corresponding to the values on x- and y-axes and the standard deviation constituting a constant proportion, 0.35, of the corresponding mean values. Values of other parameters are given in Table 1.

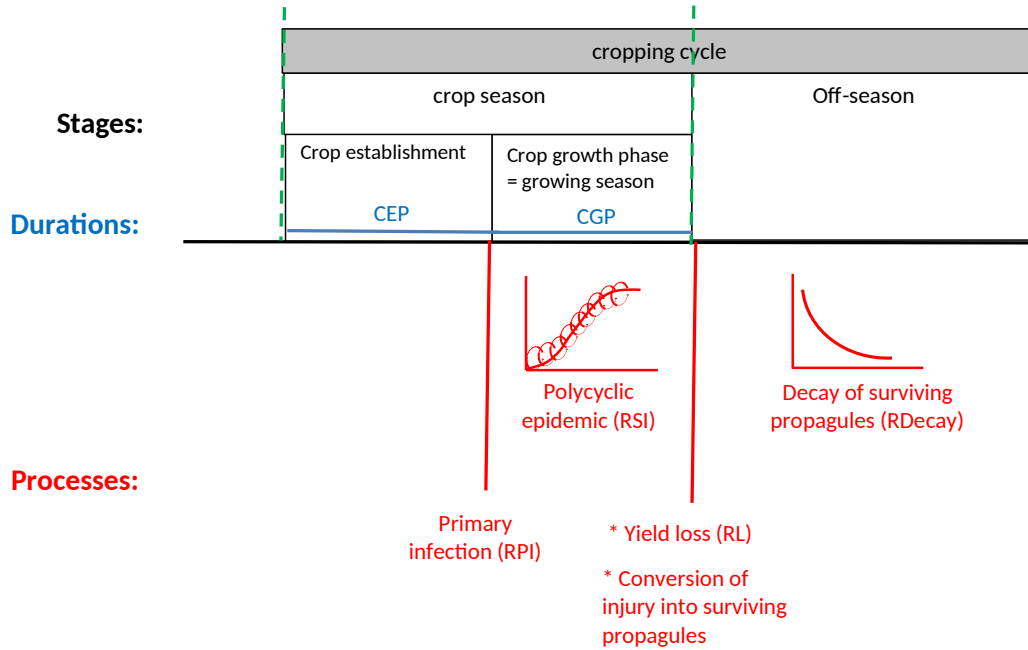
In each panel, the grey diagonal line shows the analytical threshold according to Eq. (7). Dashed black lines indicate the fitness values of the resident strain: vertical $RRg_1=0.07 \text{ day}^{-1}$; horizontal $RRD_1=0.01 \text{ day}^{-1}$. Dashed yellow lines mark the parameter regions explored in Fig. 4: $RRD_2=0.02 \text{ day}^{-1}$ in Fig. 4a, c, e; $RRg_2=0.1 \text{ day}^{-1}$ in Fig. 4b, d, f.

Crop operations:

Planting

Harvest

Planting



Supplementary Figure 1. Main stages and processes considered in the polyetic model at each

cropping cycle. CEP: duration of the Crop Establishment Phase; CGP: duration of Crop Growth phase.